Sonification of Optically-Ordered Brownian Motion

Chad McKell
Department of Physics
Wake Forest University
chadmckell@alumni.wfu.edu

ABSTRACT

In this paper, a method is outlined for the sonification of experimentally-observed Brownian motion organized into optical structures. Sounds were modeled after the tracked, three-dimensional motion of Brownian microspheres confined in the potential wells of a standing-wave laser trap. Stochastic compositions based on freely-diffusing Brownian particles are limited by the indeterminacy of the data range and by constraints on the data size and dimensions. In this study, these limitations are overcome by using an optical trap to restrict the random motion to an ordered stack of two-dimensional regions of interest. It is argued that the confinement of the particles in the optical lattice provides an artistically appealing geometric landscape for constructing digital audio effects and musical compositions based on experimental Brownian motion. A discussion of future work on data mapping and computational modeling is included. The present study finds relevance in the fields of stochastic music and sound design.

1. INTRODUCTION

In his 1956 work *Pithoprakta* [1], Greek composer Iannis Xenakis modeled a sequence of glissandi after the random walk of Brownian particles in a fluid [2]. Specifically, he assigned values from a Maxwell-Boltzmann distribution of particle speeds to the pitch changes of 46 solo strings. The sequence was unique because it converted an intrinsic aspect of stochastic motion, namely the chance variation in speed between particle collisions [1], to audible sound.

Pioneered by Xenakis, stochastic music represented a slight departure from the indeterminate music written earlier by American composers Charles Ives, Henry Cowell, and John Cage [3]. In *Pithoprakta*, indeterminacy was present in the individual mappings of each instrument, but, as a group, the mappings modeled well-defined laws of probability. In this sense, the composition was both random and deterministic. Although the mappings were also physically-informed, Xenakis appeared to be guided more by statistical descriptions of Brownian motion rather than theoretical diffusion equations or experimental observations of the phenomenon. Moreover, the physical values

---

[1] Although the distribution of speeds was Gaussian, the time intervals used to define the speeds, or glissandi of each instrument, appear to have been imposed arbitrarily [2, Fig. I–7].

that defined the motion were modified to accommodate the constraints of a live orchestra. For example, each three-dimensional velocity vector was reduced to a directionless value of speed from which the glissando of an individual instrument could be deduced.

In the present study, an optical trapping setup was implemented in hopes of better harnessing the experimentally-observed nature of Brownian motion for use in data sonification and sound design. An element of determinism was incorporated into the compositional technique by restricting individual stochastic trajectories to user-controlled data-mapping regions. In Section 2, the principles governing the Brownian motion of freely-diffusing and optically-ordered particles are outlined and compared. In Section 3, a historical overview of optical trapping configurations is provided in order to motivate the necessity of a standing-wave optical trap for purposes of surface isolation and data variety. In Section 4, the experimental methods are briefly outlined. In Section 5, the data sonification is described in detail. Finally, the paper concludes with a discussion of future research on data-mapping designs and computational modeling for real-time data sonification.

2. BROWNIAN MOTION

2.1 Freely-Diffusing Particles

The equation of motion for the finite trajectory of a freely-diffusing Brownian particle of mass M in a uniform viscous fluid is [4]

$$M\ddot{\mathbf{r}} = -\gamma\dot{\mathbf{r}} + \sqrt{2\gamma k_{\mathrm{B}}T}\Gamma(t), \qquad (1)$$

where γ is the fluid drag coefficient, k_{B} is Boltzmann's constant, T is the temperature of the fluid, $\Gamma(t)$ is the zero-average Gaussian white noise, and $\mathbf{r} = x(t)\hat{x} + y(t)\hat{y} + z(t)\hat{z}$ is the particle's position as a function of time t. By "freely-diffusing", it is understood that the particle's trajectory is only determined by the molecular interactions with the background medium, assuming the walls of the fluid chamber are sufficiently far away from the particle and evaporation of the fluid is negligible. Since the inertial term $M\ddot{\mathbf{r}}$ is small compared to the drag term $\gamma\dot{\mathbf{r}}$ in a viscous fluid, the inertial term can be dropped from Eq. (1). This simplification gives the following solution [2] for the velocity $\dot{\mathbf{r}}$ of the particle as a function of time t:

$$\dot{\mathbf{r}} = \sqrt{2D}\Gamma(t). \qquad (2)$$

---

[2] The system described by Eq. (2) is said to exhibit "overdamped" behavior since the viscous damping overpowers the inertial acceleration.

Here, D is the theoretical diffusion coefficient defined by Einstein's formula:

$$D = \frac{k_{\mathrm{B}}T}{\gamma}. \qquad (3)$$

Absent any external force, the particle will amble indefinitely through the fluid in an indeterminate manner. A sonification scheme based on the experimental position data of a freely-diffusing Brownian particle, as characterized above, is limited in at least three ways: (1) the range of data values is generally unpredictable; (2) the collected data will be sparse given the experimental state of the art for imaging unbounded Brownian microparticles; and (3) the data will be limited to two dimensions, barring the use of a sophisticated method for measuring vertical displacement from the imaging plane. In other words, there is an undesirable indeterminacy on the physical range of values obtained for mapping the audible parameters as well as constraints on the size and dimensions of the data. In an ideal scenario, however, the composer would have some control over the range of values along with ample and varied data to choose from.

To remedy these shortcomings, the particle's motion was confined to manageable regions of study by adding an optical-trapping potential $V(\mathbf{r})$ to the system.

2.2 Optically-Ordered Particles

Inserting the diffusion coefficient D and the trapping potential $V(\mathbf{r})$ into Eq. (1) gives the following time-varying solution for the velocity $\dot{\mathbf{r}}$ of an optically-trapped (i.e. "optically-ordered") Brownian particle in a viscous fluid:

$$\dot{\mathbf{r}} = -\frac{\nabla V(\mathbf{r})}{\gamma} + \sqrt{2D}\Gamma(t). \qquad (4)$$

As in Eq. (2), the inertial term $M\ddot{\mathbf{r}}$ was omitted to reflect the overdamped nature of the motion. The confining potential $V(\mathbf{r})$ is defined by [5]

$$V(\mathbf{r}) = -n\alpha\frac{|\mathbf{E}(r,z)|^2}{2}, \qquad (5)$$

where n is the refractive index of the background viscous fluid, α is the polarizability of the particle, $r = \sqrt{x^2 + y^2}$ is the particle's lateral displacement from the z-axis, and $|\mathbf{E}(r,z)|^2$ is the magnitude squared of the total electric field of the optical beam. The total field irradiance $I(r,z)$ of the beam is proportional to the total electric field by the relation [5]

$$I(r,z) = \frac{\varepsilon_0 c_0}{2}|\mathbf{E}(r,z)|^2, \qquad (6)$$

where ε_0 is the electric permittivity of free space and c_0 is the speed of light in vacuum. Along a two-dimensional trapping plane of the optical field, the solution for the velocity $\dot{\mathbf{r}}$ of the particle becomes

$$\dot{\mathbf{r}} = \frac{n\alpha\nabla_\perp I(r,h)}{\varepsilon_0 c_0\gamma} + \sqrt{2D}\Gamma(t), \qquad (7)$$

where $\nabla_\perp I(r,h)$ is the transverse irradiance gradient of the laser beam along the $z = h$ trapping plane. The following finite-difference algorithm can be implemented to solve this stochastic differential equation numerically for

the positions $\mathbf{r}_i = [x_i, y_i, h]$ as a function of the times $t_i = i\Delta t$ [6]:

$$\mathbf{r}_i = \mathbf{r}_{i-1} + \frac{n\alpha\nabla_\perp I(r,h)}{\varepsilon_0 c_0\gamma}\Delta t + \sqrt{2D\Delta t}\mathbf{w}_i. \qquad (8)$$

Here, i is the iteration of the finite-difference simulation, Δt is the time step, and $\mathbf{w}_i$ is a vector of Gaussian random numbers with unit variance and zero mean. In the next section, a brief overview of the historical development of optical traps is provided in order to elucidate the advantages of using a standing-wave optical trap to analyze Brownian motion compared with other trapping models.

3. AN OPTICAL TRAPPING ODYSSEY

3.1 Particle Acceleration and Confinement

The acceleration of matter by radiated light pressure was first explained by Johannes Kepler in 1619 [7]. Due to the immense irradiance of light emitted by the sun, Kepler observed that the gas and minerals of a comet could be pushed by the light. In 1873, James Maxwell discovered that the radiated light pressure P was equal to the time-averaged field irradiance I of the light divided by the speed of light c [8]. In theory, light radiation pressure could be used to accelerate particulate matter on Earth, assuming the irradiance of the light was substantially large compared to the magnitudes of the perturbed masses.

With the invention of high-irradiance lasers in 1960 [9], light radiation pressure could be feasibly applied to the acceleration and confinement of microscopic-sized particles. The first laser trap was developed in 1970 by Arthur Ashkin at Bell Laboratories [10]. It consisted of two counter-propagating, coaxial Gaussian beams focused at points upstream from their plane of intersection, as shown in Fig. 1. A microsphere located inside the optical field of the two beams was pulled toward the propagation axis (i.e. z-axis) by a transverse gradient force $\mathbf{F}_{\mathrm{grad}}$ and accelerated downstream by an axial scattering force $\mathbf{F}_{\mathrm{scat}}$. Together these forces tightly confined the particle at the point where the intersection plane of the beams met the propagation axis. A breakthrough in laser technology, Ashkin's trap eventually inspired the development of a wide array of trapping configurations, including optical tweezers [3].
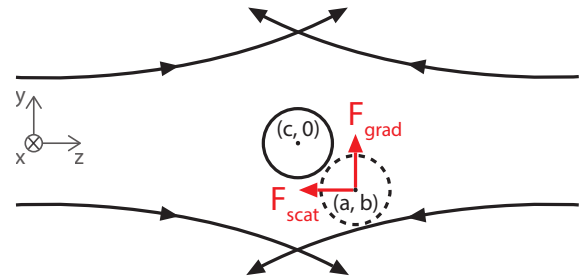

Figure 1. The first optical trap. Two opposing laser beams intersect along the $z = c$ plane. A spherical particle located at the point (a, b) in the zy-plane is pulled to the force equilibrium position $(c, 0)$ by optical forces $\mathbf{F}_{\mathrm{grad}}$ and $\mathbf{F}_{\mathrm{scat}}$. Note: The positive x-axis is into the page.

---

[3] One of the most common optical trapping designs employed by scientists today, optical tweezers are optimal for high-precision, three-dimensional manipulation of microscopic particles.

Although these early trapping designs provided a useful means for stable, surface-isolated trapping, they were not ideal for tracking Brownian motion because they either eliminated the particle's microscopic motion or complicated the imaging process. Standing-wave traps, on the other hand, allowed for enlarged, two-dimensional trapping regions that were convenient for analyzing Brownian diffusion. Additionally, the particles could move vertically from one trapping level to another, permitting a more diverse collection of data.

3.2 The Brownian Trap

The Brownian trap is a standing-wave optical trap containing a vertical lattice of individual trapping regions that are ideal for tracking transverse particle diffusion. The first standing-wave optical trap was developed in 1999 by Zemánek et al. [11]. In a typical standing-wave trapping setup, a laser beam reflects off a mirrored surface positioned perpendicular to the propagation axis and superimposes on the incident beam. The superposition of the beams produces an optical standing wave capable of simultaneous particle confinement in separate, surface-isolated [4] regions.

When fluid-immersed microspheres are introduced in the vicinity of the laser trap, optical forces pull the spheres toward the antinodes of the standing wave, enclosing them in two-dimensional optical pockets [5]. Assuming the counter-propagating beams of the standing-wave trap are well-aligned, the spheres primarily [6] experience an axial gradient force $\mathbf{F}_X$ and a transverse gradient force $\mathbf{F}_{grad}$. By analogy to gravity, the optical barriers induced by $\mathbf{F}_X$ and $\mathbf{F}_{grad}$ confine a single microsphere along a particular antinode like a marble in a bowl, as depicted in Fig. 2. Due to molecular interactions with the fluid, the particle may jump in and out of the trap. However, the barriers tend to contain the motion within the optical field.

With test particles captured in the confinement regions of the Brownian trap, one can record the positions of the particles over time using experimental imaging and tracking tools. The tracked points can then be mapped to audible parameters to create a data sonification of experimental Brownian motion.
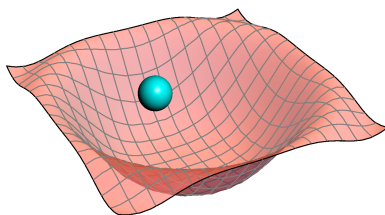

Figure 2. Force field analogy. The optical force field encountered by a microsphere at an antinode of the Brownian trap is similar to the gravitational field experienced by a marble rolling in a bowl.

---

[4] Surface isolation simplifies the motion by eliminating surface drag.

[5] Refer to Fig. 4 for an illustration of a standing-wave optical trap. Note that the trapping regions (dotted lines) lie along the antinodal planes.

[6] The reflective surface may transmit some laser light for imaging purposes. In such cases, a net axial scattering force $\mathbf{F}_{scat}$ oriented downstream is also present in the trap, shifting the trapping planes slightly downstream from the antinodal planes.

4. EXPERIMENTAL SETUP

To obtain tracking data of experimental Brownian motion, fluorescent microspheres were inserted into the optical field of a Brownian trap [7]. The particles were imaged with a CCD camera at a rate of 15 frames per second. Video files of individually trapped particles were analyzed using video tracking software in order to determine the horizontal (x, y) positions of each particle over time. The data sets ranged from 98 to 1690 points. The horizontal magnitudes r_i of the displacement vectors $\mathbf{r}_i$ at each time t_i were subsequently calculated. The vertical displacements z_i were determined based on the sizes of the diffraction patterns produced by the diffusing fluorescent spheres relative to a measured standard [8]. In the following section, the data-mapping scheme used to sonify the horizontal and vertical displacements is outlined. Web addresses containing audio samples of the sonified data are also provided.

5. DATA SONIFICATION

5.1 Audio Samples

To hear samples of the data sonification, email the author or visit brownian.bandcamp.com. Audio-visual samples are also available online at youtube.com/chadmckell and vimeo.com/brownian.

5.2 Horizontal Dynamics

5.2.1 Equal-Area Mapping

The radial displacements r_i of individual Brownian particles were mapped to specific notes on a selected musical scale for every time t_i (see Fig. 3). To sonify the horizontal data, two data-mapping approaches were implemented—equal-area and biased mapping. In equal-area mapping, the total area [9] of the trapping region was divided into sub-regions of equal area $A_E = \pi/8 \ \mu m^2$, as plotted in Fig. 3 (middle). Each sub-region corresponded to a unique MIDI note number m_i on a particular scale. In the chromatic scale on C, for example, an r value in the range $(0 \leq r < \sqrt{8}/8) \ \mu m$ mapped to C4 ($m = 60$); an r value in the range $(\sqrt{8}/8 \leq r < 1/2) \ \mu m$ mapped to C#4 ($m = 61$); and so forth.

Mapping algorithms were programmed in Java to determine the MIDI note numbers m_i for every displacement r_i measured at time t_i. The computed note arrays $\{m_1, m_2, m_3...\}$ were then inserted into Pure Data (Pd) and sampled at a rate [10] of 15 Hz (900 beats per minute). Reverberated sine waves were generated using objects osc~ and freeverb~ in Pd. Files containing the MIDI note arrays and Pd patches are available from the author on request.

---

[7] A detailed description and analysis of the laboratory setup is available in Ref. [5]. Information is included about the physical parameters of the laser and other optical components, the measured distances between the components, the sizes and material composition of the spheres, and the experimental tools used to collect and analyze videos of trapped particles.

[8] See [5, pp. 57–61].

[9] The total area of the trapping region varied depending on the maximum horizontal displacement from the origin.

[10] A sampling rate of 15 Hz was chosen in order to match the frame rate of the imaging camera.
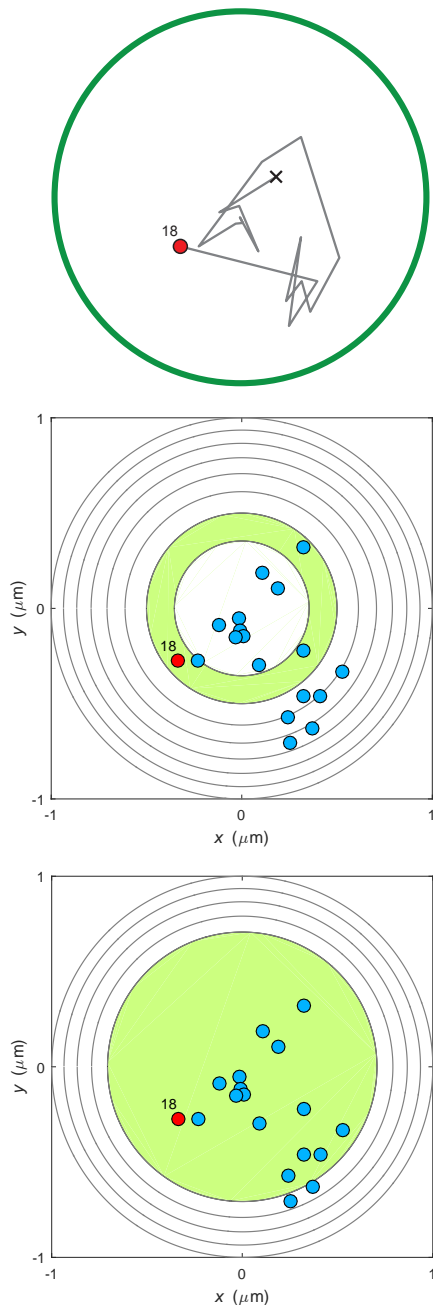
Figure 3. Data-mapping scheme—horizontal dynamics. Top: Each radial displacement r_i of a trapped microsphere mapped to an audible pitch. As the sphere moved from its starting point ("×") to its ending point ("18") in 18 steps, the pitch was updated 18 times at a sampling rate of 15 Hz. Middle (*equal-area mapping*): The total area of the trapping region was divided into sub-regions of equal area. In the example depicted here, the radial points in each sub-region mapped to a unique MIDI note number m_i in the chromatic scale on C. The ending point ("18") mapped to C#4 since it was located in the second sub-region (shaded area) from the origin. Bottom (*biased mapping*): the area of the centermost sub-region was increased to encircle the majority of the radial points. The new mapping reassigned the ending point ("18") to the centermost sub-region (shaded area) so that the point charted to C4.

5.2.2 Biased Mapping

Biased data mapping allows the composer to increase the stability of the centermost (i.e. lowest-frequency) note while retaining the stochastic nature of higher-pitched note combinations. In this mapping approach, the area of the centermost sub-region is enlarged in order to increase the

probability that a given r value will lie within the centermost sub-region. In Fig. 3 (bottom), the area of the centermost sub-region was increased to $A_B = \pi/2$ μm^2 so that, in the chromatic scale on C, an r value in the range $(0 \leq r < \sqrt{2}/2)$ μm mapped to C4. Each remaining sub-region retained an area of $A_E = \pi/8$ μm^2 so that an r value in the range $(\sqrt{2}/2 \leq r < 2\sqrt{10}/8)$ μm mapped to C#4; an r value in the range $(2\sqrt{10}/8 \leq r < \sqrt{3}/2)$ μm mapped to D4; and so forth.

5.2.3 Multiple Particles

Single particle sonifications were summed in Pd in order to hear the individual stochastic trajectories en masse. Chordal harmonies were created by charting the centermost sub-region of each trajectory to a different note in a chosen scale. While dissonant, equal-area mapping more accurately portrayed the movements of each particle near the origin of the tracking grid. Biased mapping, on the other hand, allowed for more musical consonance.

5.3 Vertical Dynamics

The three-dimensional [11] nature of the tracking data emerged when transitions between trapping planes were measured. As the fluorescent microspheres moved from one trapping pocket to another, fluorescent light from the spheres diffracted through the imaging apparatus. The sizes of these diffraction patterns were compared to a measured standard in order to determine the discrete, vertical displacements z_i of the particles. One possible mapped trajectory of a particle moving vertically in the trap is illustrated in Fig. 4.

To sonify the vertical jumps z_i, the mapping region (i.e. the range of mapped notes) was shifted by one octave for every unit transition along the lattice. For example, if a microsphere dropped down two trapping levels, the mapping region transposed down two octaves; if the particle jumped up one trapping level, the region moved up one octave.
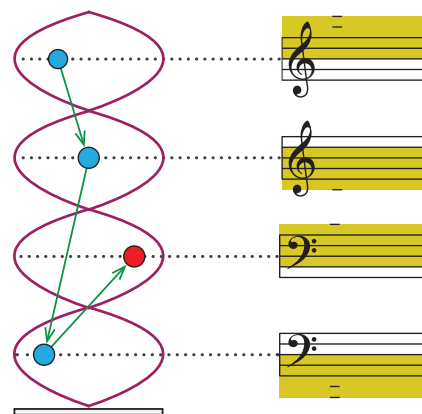

Figure 4. Data-mapping scheme—vertical dynamics. A transition of one antinode along the standing wave transposed the mapping region (shaded area on the staff) by one octave. In the scenario shown here, the trajectory caused a shift of one octave down, then two octaves down, then one octave up. Note: each mapping region in this example spanned one octave in the chromatic scale on C. In practice, however, a typical mapping region covered several octaves.

[11] The three dimensions are represented by the cylindrical coordinates r, θ, and z. Mapping the polar coordinate θ is reserved for future work.

6. FUTURE DIRECTIONS

6.1 Data Mapping

In order to extract more artistic value from the experimental tracking data discussed in this paper, future work on data mapping is proposed. The data-mapping scheme outlined in Section 5 is one among many possible methods. In addition to pitch, the calculated displacements [12] may be mapped to other audible variables, such as timbre and amplitude panning. In two-dimensional vector base amplitude panning (VBAP) [12], the gain factors g_i of individual loudspeakers in a circular array could fluctuate in accordance with a particle's position inside a trapping region, as depicted in Fig. 5. Assigning different values to the sampling rate [13] and the mapping areas A_E and A_B may also be explored. Additionally, other optical trapping setups, aside from standing-wave traps, could be devised. Maximizing the complexity of these trapping configurations would be particularly desirable since a more intricate setup would lend more options for mapping the data.
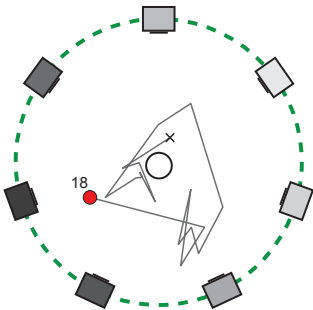

Figure 5. Two-dimensional VBAP. A listener (white circle) perceives higher gain factors g_i (darker shading) from loudspeakers located closer to a particle's mapped position ("18"). Note: the trapping region (dashed border) was scaled to match the size of the circular loudspeaker array.

6.2 Computational Modeling

Given values for each of the physical variables in Eq. (8), a computer program can be written to generate a continuous stream of Brownian position data for real-time sonification and manipulation. In a model based on the equation of motion of an optically-ordered Brownian particle, the composer would adjust the parameters of the "Brownian" audio effect by altering the physical parameters of the particle, the Brownian trap, or the background fluid environment. Increasing the transverse irradiance gradient $\nabla_\perp I(r, h)$ of the laser, for example, would make the particle more likely to reside in the centermost sub-region and less likely to escape the trap. Such a change would increase the stability of the lowest-frequency note and reduce the likelihood of higher-pitched, stochastic sequences. Increasing the fluid viscosity γ, moreover, would slow the particle's average velocity, effectively increasing the duration over which notes were played. Data-mapping algorithms could also be incorporated into the model to manipulate the sampling rate and mapping areas in real time.

---

[12] Apart from displacement, other physical observables, such as average velocity, may be computed from the tracking data and then sonified.

[13] Although the sonification would no longer accurately reflect the physical scenario observed in the laboratory, changing the sampling rate to mismatch the imaging rate may be of artistic interest.

7. CONCLUSION

Data sonifications based on optically-ordered Brownian motion benefit from the fact that the data range can be controlled and the data size and dimensions can be maximized. In this study, a standing-wave optical trap was used to restrict the random motion of diffusing Brownian microspheres to an ordered stack of two-dimensional trapping planes. It was shown that the arrangement of the particles in the lattice provided an attractive framework for producing diverse and manageable sonification data. Lastly, a discussion of potential avenues for research in data mapping and computational modeling was included in order to propel the ideas outlined in the paper.

8. ACKNOWLEDGMENTS

9. REFERENCES

[1] I. Xenakis, *Pithoprakta*. Boosey & Hawkes, 1967.

[2] ——, *Formalized Music: Thought and Mathematics in Composition*. Pendragon Press, 1992.

[3] P. Griffiths, "Aleatory," *The New Grove Dictionary of Music and Musicians*, vol. 1, 2001.

[4] D. Gillespie and E. Seitaridou, *Simple Brownian Diffusion: An Introduction to the Standard Theoretical Models*. Oxford University Press, 2012.

[5] C. McKell, *Confinement and Tracking of Brownian Particles in a Bessel Beam Standing Wave*. Master's Thesis, Wake Forest University, 2015.

[6] G. Volpe and G. Volpe, "Simulation of a Brownian particle in an optical trap," *American Journal of Physics*, vol. 81, no. 3, pp. 224–230, 2013.

[7] J. Kepler, *De cometis libelli tres*, 1619.

[8] J. C. Maxwell, *A treatise on electricity and magnetism*, 1st ed. Clarendon Press, 1873.

[9] T. H. Maiman, "Stimulated optical radiation in ruby," *Nature*, 1960.

[10] A. Ashkin, "Acceleration and trapping of particles by radiation pressure," *Physical Review Letters*, vol. 24, no. 4, pp. 156–159, 1970.

[11] P. Zemánek, A. Jonáš, L. Šrámek, and M. Liška, "Optical trapping of nanoparticles and microparticles by a Gaussian standing wave," *Optics Letters*, vol. 24, no. 21, pp. 1448–1450, 1999.

[12] V. Pulkki, "Virtual sound source positioning using vector base amplitude panning," *Journal of the Audio Engineering Society*, vol. 45, no. 6, pp. 456–466, 1997.